Ordering of polarons in the charge-disordered phase of $Pr_{0.7}Ca_{0.3}MnO_3$

A. Levstik, C. Filipič, V. Bobnar, A. Potočnik, D. Arčon, S. Drnovšek, and J. Holc
Jožef Stefan Institute, Jamova 39, 1000 Ljubljana, Slovenia

Z. Jagličić
Institute of Mathematics, Physics, and Mechanics, Jadranska 19, 1000 Ljubljana, Slovenia and Faculty of Civil and Geodetic Engineering, University of Ljubljana, Jamova 2, 1000 Ljubljana, Slovenia

(Received 12 December 2008; revised manuscript received 9 April 2009; published 30 April 2009)

$Pr_{1-x}Ca_xMnO_3$ (PCMO, x=0.3) ceramic is a member of the manganite family that exhibits a colossal magnetoresistance. We report a comprehensive study of perovskite manganite PCMO (x=0.3) ceramic with EPR, dielectric spectroscopy, and ac electrical conductivity. Activated-type temperature dependence of EPR linewidth is a strong signature for a hopping of Jahn-Teller polarons above ≈150 K. Analysis of the electrical conductivity and dielectric constant data suggests the ordering of polarons in the charge-disordered state of PCMO (x=0.3) below 60 K. This provides a new understanding of the phase diagrams in PCMO systems.

DOI: 10.1103/PhysRevB.79.153110 PACS number(s): 73.40.Gk, 71.38.−k, 71.30.+h, 75.47.Lx

The observation of colossal magnetoresistance (CMR) effects in perovskite manganite films[1–3] has stimulated the intensive research on manganese oxides. $LaMnO_3$, the prototype compound of this family, is an antiferromagnetic insulator characterized by a strong structural distortion, interpreted in terms of a cooperative Jahn-Teller (JT) effect. On partial substitution of La with a divalent alkaline-earth metal, the corresponding fraction x of Mn^{+3} is formally replaced with Mn^{+4} and, for compositions $0.2<x<0.4$, the compounds are ferromagnetic, exhibiting CMR.[3] The doped systems, with the general formula $A_{1-x}A'_xMnO_3$ (A=rare earth, A'=Ca,Sr,Ba), are characterized by strong competition between two different ground states: a charge-ordered (CO) insulating state, where Mn e_q electronic states are localized and tend to order onto separate crystallographic sublattices, and a charge-disordered (CD) state showing metalliclike dc conductivity.[4,5] Ca and Sr doped $PrMnO_3$ in particular, exhibit some spectacular effects which are still a subject of scientific debate. Various properties of PCMO ceramics have been reported,[6–8] including the following properties for PCMO (x=0.3).[9,10] The charge and orbital order has been simultaneously established at $T_{c0}\approx 200$ K. At $T_N\approx 150$ K Mn moments order into the collinear antiferromagnetic order. At $T_{CA}\approx 120$ K another magnetic transition into a weak ferromagnetic state is observed due to small canting of Mn magnetic moments. Finally, in magnetic fields, a metal to insulator transition is induced that is irreversible below 60 K.[11]

Recently it has been shown that, in PCMO in the doping range $0.2<x<0.5$, the electric transport is dominated by the hopping of small Jahn-Teller polarons with an activation energy of $W_k\approx 110-190$ meV.[12] When applying a sufficiently high current, the electrical resistivity is strongly reduced over the whole temperature range and a steplike change occurs at a percolation temperature T_p. Above T_p the temperature dependence can be described by the model for thermally activated polarons, where the activation energy decreases with increase of current to 80 meV. This current dependent activation barrier is a fingerprint of a polaron liquid. Below T_p the strong increase of $\rho(T)$ at low currents reflects the freezing out of the polaron modes. At high currents the activation energy below T_p decreases further, indicating a transition to a light polaron. The electrically induced polaron solid-liquid transition in PCMO (x=0.5) has in fact been observed by high-resolution transmission electron microscopy (TEM),[12] and the effect has been connected to CMR. It has been concluded that the electrically induced coherent polaron motion and the solid-liquid transition comprise the first step in understanding a complicated polaron phase diagram.

In the present work we report on the study of polaron dynamics of the PCMO (x=0.3) ceramics over a broad temperature interval. At high temperatures ($T>150$ K) thermally activated dependence of EPR linewidth provide evidence for JT polarons. At low temperatures temperature dependent dielectric data detects the ordering of polarons in the low-temperature CD phase of PCMO (x=0.3).

PCMO (x=0.3) powder was prepared by mechanochemical synthesis.[13] The starting materials were powders of Pr_6O_{11} (Alfa Chemicals, 99.99%), $CaCO_3$ (Alfa Chemicals, 99.95%), and MnO_2 (Alfa Chemicals, 99.9%). Synthesis was achieved in a Retsch PM 400 planetary mill working at 300 rpm for 12 h in tungsten carbide milling jar and balls. A deagglomeration treatment was accomplished for the synthesized powder by attrition milling in isopropanol for 4 h. Powder was uniaxially pressed into disks and further consolidated by isostatic pressing at 300 MPa. Ceramic with a density of 5.98 g/cm^3 was prepared by sintering at 1250 °C for 4 h in the air. The ceramic sample is phase pure according to x-ray diffraction (XRD) analysis. Gold electrodes were sputtered on the disks' surfaces. The ceramic powder sample for EPR measurements was sealed under dynamic vacuum into a 1 mm diameter capillary. Continuous wave x-band EPR measurements were performed on a commercial Bruker E580 spectrometer equipped with an Oxford Cryogenics ESR900 cryostat. Temperature stability was ±0.2 K. Typical microwave power was set to 1 mW while the modulation field was 2 G. The dc magnetic susceptibilities, χ, were measured using a commercial superconducting quantum interference device magnetometer QD-MPMSXL5. The complex dielectric constant $\varepsilon^*(\nu,T)=\varepsilon'-i\varepsilon''$ was measured between 300 and 4.5 K in the frequency range of 1 Hz to 1 MHz, using a Novocontrol Alpha high resolution dielectric

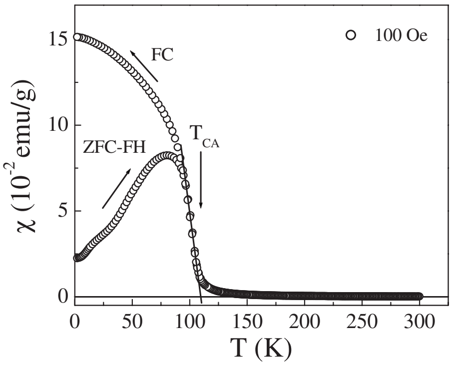

FIG. 1. Splitting between field-cooled (FC) and zero-field-cooled–field-heated (ZFC-FH) magnetic susceptibilities, revealing a phase transition at 110 K, close to the previously determined T_{CA}. χ was measured at a dc field of 100 Oe.

analyzer. The amplitude of the probing ac electric signal was 10 V/cm. The temperature was stabilized to within ± 0.1 K using an Oxford Instruments continuous flow cryostat. The real part of the complex ac conductivity $\sigma^* = \sigma' + i\sigma''$ was calculated from $\sigma' = 2\pi\nu\varepsilon_0\varepsilon''$, with ε_0 being the permittivity in vacuum.

In order to characterize our sample, the temperature dependence of the FC and ZFH-FC magnetic susceptibility was measured, which is shown in Fig. 1. χ was measured at dc magnetic field of 100 Oe. At 110 K we observe the phase transition which is close to the previously determined T_{CA}.[11]

A typical room-temperature X-band EPR spectrum is shown in the inset to Fig. 2. The EPR line shape can be well simulated by a single Lorentzian line shape with a room-temperature linewidth $\Delta H_{pp} = 1584 \pm 3$ G and $g = 2.008 \pm 0.001$. On cooling, the EPR linewidth decreases and reaches a minimum at 132 K, i.e., 18 K below the antiferromagnetic transition temperature $T_N = 150$ K. Above T_N, ΔH_{pp} can be well described with an activated type temperature dependence $\Delta H_{pp} = (A/T)\exp(-E_a/kT)$ (Fig. 2). The value of the activation energy is $E_a = 42 \pm 1$ meV. A model with such a temperature dependence was suggested by

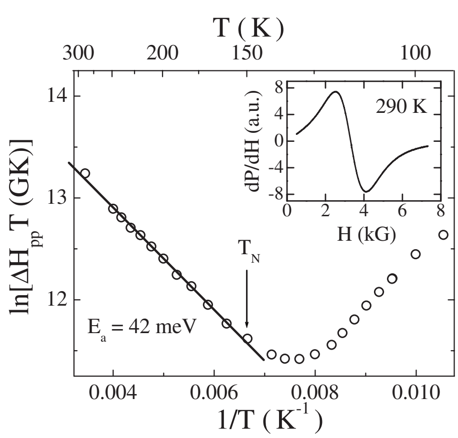

FIG. 2. The temperature dependence of $\ln(\Delta H_{pp})$ for PCMO ($x=0.3$). A representative X-band spectrum measured at room temperature is shown in the inset. Above $T_N = 150$ K, ΔH_{pp} can be well described with an activated type temperature dependence.

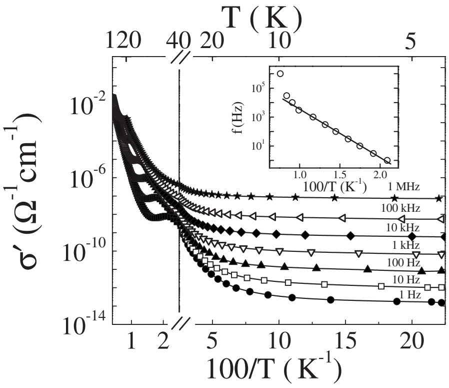

FIG. 3. The temperature dependence of the real part of the complex ac conductivity σ', measured at several frequencies. In order to reveal the high-temperature behavior, the data above 40 K are presented in a rescaled range (left part) in comparison to those detected below 40 K (right part). The inset shows the relaxation frequency determined from the peaks in $\sigma'(T)$ (in the left part) versus reciprocal temperature.

Shangelaya *et al.*[14] to describe a phase in which the spin-lattice relaxation is controlled by small Jahn-Teller polaron hopping. In the paramagnetic phase, the conductivity of manganites shows the same temperature behavior, with similar values of E_a.[14,15] On further cooling below 132 K, ΔH_{pp} starts to increase rapidly and, due to critical fluctuations, almost diverges. In the same temperature interval the g factor also starts to shift to higher values, due to the short-range order effects. Below 132 K a very broad and asymmetric resonance was measured, reflecting large local magnetic fields in the magnetically ordered phase.

Besides infrared excitation in optical conductivity,[16,17] the fingerprint of polarons is usually connected with the temperature and frequency dependence of ac electrical conductivity.[18–20] The ac electrical conductivity of $Pr_{0.7}Ca_{0.3}MnO_3$ was measured as a function of temperature at several frequencies (Fig. 3). The observed behavior is typical of the existence of polarons in the system: while at higher temperatures σ' is strongly temperature dependent, below 30 K the conductivity becomes almost independent of the temperature. The data above 40 K are presented in a rescaled range (left part of Fig. 3) in comparison to those detected below 40 K (right part of Fig. 3). One can thus clearly see that below 30 K the conductivity is almost independent of the temperature while at higher temperatures σ' becomes strongly temperature dependent. From the maxima in $\sigma'(T,\nu)$ we plotted the relaxation frequency versus reciprocal temperature (inset to Fig. 3). Arrhenius plot is valid from approximately 40 K until $T_{CA} \approx 120$ K. Below 30 K the $\sigma'(T)$ plateaus are strongly frequency dependent, which suggests that hopping or tunneling of localized charge carriers governs the electrical transport at low temperatures.[21]

The frequency dependence of the ac electrical conductivity in PCMO ($x=0.3$) is shown in Fig. 4(a). At lower frequencies, $\sigma'(\nu)$ curves start to saturate toward the dc conductivity. At higher frequencies, on the other hand, σ' follows a power law $\sigma' = \sigma_1 \nu^n$ with $n \approx 1$ and, for the lowest temperatures, such behavior was observed over a broad fre-

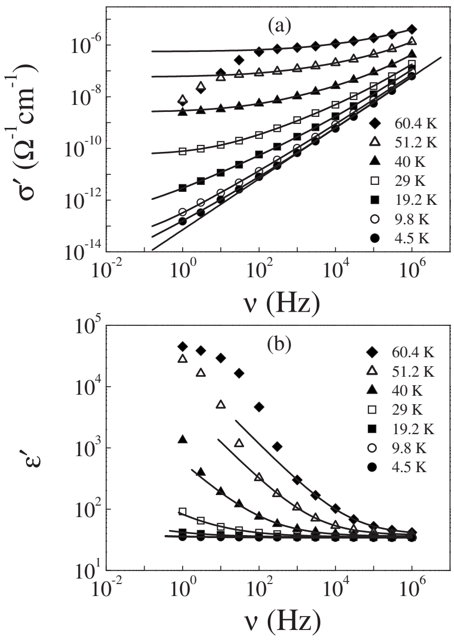

FIG. 4. (a) Frequency dependence of the electrical conductivity σ' at selected temperatures. The solid lines are fits, performed simultaneously for σ' and ε', with an expression combining a dc contribution, a UDR hopping contribution, a ν^n power law, and a limiting high-frequency dielectric constant ε_∞. (b) Frequency dependence of the real part of the complex dielectric constant at various temperatures. Solid lines are the simultaneous fits of σ' and ε' with the same contributions as in Fig. 4(a).

quency range of four decades. It is however known[22] that a simple ansatz $\sigma'(\nu)=\sigma_{dc}+\sigma_1\nu^n$ must be replaced in some substances, such as in $Pr_{0.65}Ca_{0.28}Sr_{0.07}MnO_3$, by the additional presence of a sublinear increase, $\sigma'=\sigma_0\nu^s$ with $s<1$. This contribution, a so-called universal dielectric response (UDR), is predicted by various models,[23] and the resulting expression for the frequency dependent electrical conductivity is thus $\sigma'(\nu)=\sigma_{dc}+\sigma_0\nu^s+\sigma_1\nu^n$. The expression for the frequency dependence of the dielectric constant, $\varepsilon'(\nu)=\varepsilon_\infty+\varepsilon_0\nu^{s-1}+\varepsilon_1\nu^{n-1}$, is obtained by the Kramers-Kronig transformation. The solid lines in Figs. 4(a) and 4(b) are obtained by simultaneous fits of the experimental $\sigma'(\nu)$ and $\varepsilon'(\nu)$ data to the above expressions.

The UDR exponent s was determined by the above mentioned fitting procedure as a function of the temperature, for $E_{dc}=0$ and $E_{dc}=0.5$ kV/cm (Fig. 5). The applied dc electric field obviously does not affect values of the UDR exponent, which has a monotonous behavior. Such a behavior is predicted by the tunneling polaron model (originally this model was developed for the tunneling of overlapping large polarons,[23] but it was argued later[24] that it is in fact applicable to small polarons), which yields the temperature dependence of s as[23]

$$s = 1 - \frac{4 + 6W_\infty r_0'/(kTR'^2)}{R'[1 + W_\infty r_0'/(kTR'^2)]^2}. \qquad (1)$$

Here, W_∞ denotes the energy barrier and r_0' the reduced polaron radius. The reduced tunneling distance R' is also a

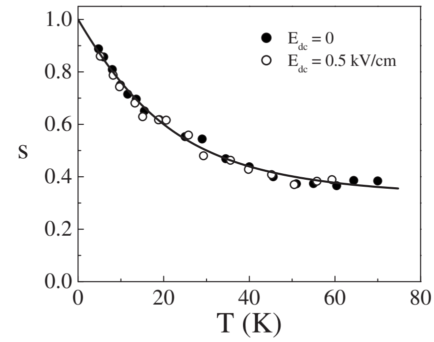

FIG. 5. The temperature dependence of the UDR parameter s determined from the fits of σ' and ε' [as presented in Figs. 4(a) and 4(b)], obtained in the absence of a dc electric field as well as in $E_{dc}=0.5$ kV/cm. The solid line is a fit to a model for polaron tunneling [Eqs. (1) and (2)].

function of W_∞ and r_0' and, additionally, of the inverse attempt frequency τ_0 as[23]

$$2R' = \ln\frac{1}{\omega\tau_0} - \frac{W_\infty}{kT} + \left(\left[\ln\frac{1}{\omega\tau_0} - \frac{W_\infty}{kT}\right]^2 + \frac{4r_0'W_\infty}{kT}\right)^{1/2}, \qquad (2)$$

where $\omega=2\pi\nu$. The fit of the experimental data below $\approx$60 K to Eqs. (1) and (2) (the solid line in Fig. 5) yields values of $W_\infty=0.019\pm0.002$ eV, $r_0'=3.6\pm0.3$, and $\tau_0=4.4\times10^{-7}$ s.

From the detected $\sigma'(\nu,T)$ and $s(T)$ data we can thus conclude that, in the CD phase below 60 K, the tunneling of polarons governs the charge transport in PCMO (x=0.3). As the dc electric field does not influence small polarons below 60 K, we believe that they are frozen in, i.e., we believe that there exist short-range correlations of ordered polarons. Similar effect, however on the long-range scale, namely, the formation of the orbital polaron lattice (OPL), has recently been observed in $La_{1-x}Sr_xMnO_3$ (LSMO) by resonant x-ray scattering at the metal-insulator transition in this compound.[25] The OPL is a clear manifestation of the strong orbital-hole interactions, which play an important role in the CMR effect in doped manganites in general. In the same paper the formation of the OPL is predicted also for PCMO. It has furthermore been proposed that the insulating state at low temperatures in PCMO (x=0.3) should be regarded as a polaron lattice.[26]

In conclusion, the temperature dependence of the EPR linewidth in PCMO (x=0.3) ceramics shows that, above 150 K, spin-lattice relaxation is controlled by small Jahn-Teller polaron hopping. In addition, with the fingerprint method of polarons, freezing in of small polarons was detected below 60 K in the charge-disordered phase. Detected ordering of polarons provides a new understanding of the phase diagrams in PCMO systems and is a clear manifestation of the strong orbital-hole interactions that play a crucial role in the CMR effect in doped manganites.

This research was supported by the Slovenian Research Agency (Grant No. P1-0125).

[1] K. Chahara, T. Ohno, M. Kasai, and Y. Kozono, Appl. Phys. Lett. **63**, 1990 (1993).
[2] R. von Helmolt, J. Wecker, B. Holzapfel, L. Schultz, and K. Samwer, Phys. Rev. Lett. **71**, 2331 (1993).
[3] S. Jin, T. H. Tiefel, M. McCormack, R. A. Fastnacht, R. Ramesh, and L. H. Chen, Science **264**, 413 (1994).
[4] P. Schiffer, A. P. Ramirez, W. Bao, and S.-W. Cheong, Phys. Rev. Lett. **75**, 3336 (1995).
[5] H. Y. Hwang, S.-W. Cheong, P. G. Radaelli, M. Marezio, and B. Batlogg, Phys. Rev. Lett. **75**, 914 (1995).
[6] Z. Jirák, S. Krupička, V. Nekvasil, E. Pollert, G. Villeneuve, and F. Zounová, J. Magn. Magn. Mater. **15-18**, 519 (1980).
[7] E. Pollert, S. Krupika, and E. Kuzmiová, J. Phys. Chem. Solids **43**, 1137 (1982).
[8] Z. Jirák, S. Krupička, Z. Šimša, M. Dlouhá, and S. Vratislav, J. Magn. Magn. Mater. **53**, 153 (1985).
[9] H. Yoshizawa, H. Kawano, Y. Tomioka, and Y. Tokura, Phys. Rev. B **52**, R13145 (1995).
[10] D. E. Cox, P. G. Radaelli, M. Marezio, and S.-W. Cheong, Phys. Rev. B **57**, 3305 (1998).
[11] Y. Tomioka, A. Asamitsu, H. Kuwahara, Y. Moritomo, and Y. Tokura, Phys. Rev. B **53**, R1689 (1996).
[12] Ch. Jooss, L. Wu, T. Beetz, R. F. Klie, M. Beleggia, M. A. Schofield, S. Schramm, J. Hoffmann, and Y. Zhu, Proc. Natl. Acad. Sci. U.S.A. **104**, 13597 (2007).
[13] D. Kuscer, J. Holc, M. Kosec, and A. Meden, J. Am. Ceram. Soc. **89**, 3081 (2006).
[14] A. Shengelaya, G. M. Zhao, H. Keller, K. A. Muller, and B. I. Kochelaev, Phys. Rev. B **61**, 5888 (2000).
[15] D. C. Worledge, G. Jeffrey Snyder, M. R. Beasley, T. H. Geballe, R. Hiskes, and S. DiCarolis, J. Appl. Phys. **80**, 5158 (1996).
[16] D. Emin, Phys. Rev. B **48**, 13691 (1993).
[17] C. Hartinger, F. Mayr, A. Loidl, and T. Kopp, Phys. Rev. B **73**, 024408 (2006).
[18] N. F. Mott and E. A. Davis, *Electronic Processes in Non-Crystalline Materials* (Oxford University Press, New York, 1979).
[19] M. Dumm, P. Lunkenheimer, A. Loidl, B. Assmann, H. Homborg, and P. Fulde, J. Chem. Phys. **104**, 5048 (1996).
[20] B. I. Shklovskii and A. L. Efros, *Electronic Properties of Doped Semiconductors* (Springer-Verlag, Berlin, 1984).
[21] R. D. Gould and A. K. Hasan, Thin Solid Films **223**, 334 (1993).
[22] J. Sichelschmidt, M. Paraskevopoulos, T. Brando, R. Wehn, D. Ivannikov, F. Mayr, K. Pucher, J. Hemberger, A. Pimenov, H.-A. Krug von Nidda, P. Lunkenheimer, V. Yu. Ivanov, A. A. Mukhin, A. M. Balbashov, and A. Loidl, Eur. Phys. J. B **20**, 7 (2001).
[23] S. R. Elliott, Adv. Phys. **36**, 135 (1987).
[24] M. P. J. van Staveren, H. B. Brom, and L. J. de Jongh, Phys. Rep. **208**, 1 (1991).
[25] J. Geck, P. Wochner, S. Kiele, R. Klingeler, P. Reutler, A. Revcolevschi, and B. Buchner, Phys. Rev. Lett. **95**, 236401 (2005).
[26] V. Kiryukhin, D. Casa, J. P. Hill, B. Keimer, A. Vigliante, Y. Tomioka, and Y. Tokura, Nature (London) **386**, 813 (1997).